



HAL
open science

Modelling the effect of demographic traits and connectivity on the genetic structuration of marine metapopulations of sedentary benthic invertebrates

Mariana Padrón, Katell Guizien

► **To cite this version:**

Mariana Padrón, Katell Guizien. Modelling the effect of demographic traits and connectivity on the genetic structuration of marine metapopulations of sedentary benthic invertebrates. *ICES Journal of Marine Science*, 2016, 73 (7), pp.1935-1945. 10.1093/icesjms/fsv158 . hal-02955365

HAL Id: hal-02955365

<https://hal.science/hal-02955365v1>

Submitted on 8 Dec 2022

HAL is a multi-disciplinary open access archive for the deposit and dissemination of scientific research documents, whether they are published or not. The documents may come from teaching and research institutions in France or abroad, or from public or private research centers.

L'archive ouverte pluridisciplinaire **HAL**, est destinée au dépôt et à la diffusion de documents scientifiques de niveau recherche, publiés ou non, émanant des établissements d'enseignement et de recherche français ou étrangers, des laboratoires publics ou privés.

1 **Modelling the effect of demographic traits and connectivity on the genetic structuration of**
2 **marine metapopulations of sedentary benthic invertebrates**

3 PADRON, Mariana^{1*} and GUIZIEN, Katell¹

4 ¹ Sorbonne Universités, UPMC Univ Paris 06, CNRS, Laboratoire d'Ecogéochimie des
5 Environnements Benthiques (LECOB), Observatoire Océanologique, 66650, Banyuls sur Mer,
6 France.

7 * mpadron@obs-banyuls.fr. Observatoire Océanologique de Banyuls sur Mer. 66650 Banyuls sur
8 Mer, France. +33(0)468887394.

9

10 **Abstract**

11 The genetic structure of populations is commonly used to infer connectivity among distant
12 populations. Accounting for connectivity is essential in marine spatial planning and the proper
13 design and management of Marine Protected Areas (MPAs), given that their effectiveness depends
14 on the patterns of dispersal and colonisation between protected and non-protected areas. Here, we
15 present a spatially explicit coupled metapopulation gene flow model that simulates the effect of
16 demographic fluctuations on the allele frequencies of a set of populations. We show that in closed
17 populations, regardless of population growth rate, the maintenance of genetic diversity at the initial
18 saturating population density increases with species life expectancy as a result of density-
19 dependent recruitment control. Correlatively, at low initial population density, the time at which a
20 population begins to lose its genetic diversity is driven by recruitment success – the larger the
21 recruitment success, the quicker the genetic drift. Different spatial structures of connectivity
22 established for soft bottom benthic invertebrates in the Gulf of Lions (NW Mediterranean, France)
23 lead to very different results in the spatial patterns of genetic structuration of the metapopulation,
24 with quick genetic drift in sites where the local retention rate was larger than 2%. The effect of
25 recruitment failure and the loss of key source populations on heterozygosity confirm that transient

26 demographic fluctuations have a major effect on the maintenance of genetic diversity in a
27 metapopulation. This study highlights the role of intra-specific settlement limitations due to lack of
28 space when the effective number of breeders approaches saturating capacity, causing a strong
29 reduction of effective reproduction. The present model allows to: 1) disentangle the relative
30 contribution of local demography and environmental connectivity in shaping seascape genetics,
31 and 2) perform *in silico* evaluations of different scenarios for marine spatial planning.

32

33 **Keywords:** connectivity, metapopulation, seascape genetics, spatially explicit model, sedentary
34 benthic invertebrates, Gulf of Lions.

35

36 **Introduction**

37 Connectivity strongly impacts the dynamics and persistence of marine populations because
38 it influences key processes, from short-term demography to long-term evolution, including
39 resistance to disturbances and environmental changes. Therefore, understanding the development
40 and maintenance of connectivity patterns is essential in marine spatial planning and the proper
41 design and management of Marine Protected Areas (MPAs) (Palumbi 2004; Botsford *et al.*, 2009).
42 However, the quantitative study of connectivity and the identification of connectivity bottlenecks
43 that could compromise the ability for populations to recover after disturbances are current
44 scientific challenges (Pineda 2000; Burgess *et al.*, 2014).

45 For sedentary marine benthic species, understanding connectivity translates into
46 understanding larval dispersal, given that it is during the pelagic larval stage that the exchange of
47 individuals and genes among populations takes place (Pineda *et al.*, 2007; Cowen and Sponaugle
48 2009). Hence, to analyse the patterns of connectivity among populations and study, in more detail,
49 the mechanisms that shape and maintain connectivity patterns through time, the dispersal of
50 organisms should be taken into account (Hastings and Botsford 2006; Aiken and Navarrete 2011).

51 Different approaches have been undertaken to try to quantify dispersal and connectivity in
52 marine ecosystems. Population genetics has been one of the most frequently used tools to provide
53 direct and indirect measures of connectivity in several marine species (Hellberg *et al.*, 2002;
54 Saenz-Agudelo *et al.*, 2009; Lowe and Allendorf 2010). The dispersal potential of the larvae
55 produced by sedentary benthic species has usually correlated with gene flow and was even used as
56 a predictor of population genetic structure (Siegel *et al.*, 2003).

57 Using estimates of Pelagic Larval Duration (PLD) as a proxy to measure realised dispersal
58 distance, several studies showed that the correlation between PLD and genetic Isolation by
59 Distance (IBD) was consistent with the expectation that migration was the key factor driving the
60 genetic structuration of marine populations (Hellberg 1996; Gilg and Hilbish 2003). However,
61 recent data set reviews (Riginos *et al.*, 2011; Selkoe and Toonen 2011; Faurby and Barber 2012)
62 have now shown that the relationship between PLD and genetic structuration might be weaker than
63 previously thought.

64 The influence of several processes (e.g. larval behaviour, availability of suitable habitat,
65 and biotic interactions) can cause the patterns of population connectivity to be different from what
66 would be expected from flow integration along PLD alone (Pineda 2000; Guizien *et al.*, 2006).
67 Among these processes, settlement or recruitment regulation of dispersal alters gene flow (Pineda
68 *et al.*, 2007), in addition to the local demography. This temporal and spatial variability in the
69 strength of gene and demographic flow due to bottlenecks during larval settlement and recruitment
70 implies that there is a set of interacting processes operating across various scales, which introduces
71 complexity into the system. Therefore, inferring connectivity by only one disciplinary approach
72 (either genetic or bio-physic) does not provide the necessary information to properly describe
73 population persistence in a network of MPAs (Hastings and Harrison 1994; Marko and Hart 2011).

74 It is therefore necessary, in order to efficiently inform conservation management
75 decisions, to use tools that integrate bio-physical models with information regarding local

76 demographic traits driving genetic linkages that result from larval exchange among populations
77 (Werner *et al.*, 2007; Cowen and Sponaugle 2009). However, detecting the genetic signatures
78 caused by the transient dynamics of demographic changes remains a challenge (Alcala *et al.*,
79 2013).

80 Although genetic models incorporating larval dispersal and demographic parameters
81 have recently been developed to quantify connectivity among marine populations (Galindo *et al.*,
82 2006; Kool *et al.*, 2009; Munroe *et al.*, 2012), they have some limitations when attempting to
83 understand connectivity patterns among non-equilibrium populations. The model Galindo *et al.*
84 (2006) developed, for example, does not take into account demographic variability, as population
85 sizes were kept constant over time. The approach Kool (2009) developed, although allowing
86 changes in population size, does not account for overlapping generations but, more importantly,
87 being an Individual-Based Model (IBM), population sizes were limited to 10 individuals.
88 Recently, Munroe *et al.* (2012), presented a modelling case study for Eastern oysters in Delaware
89 Bay (USA) in which they relaxed population size limitations and assigned each population its own
90 demographic dynamics.

91 In an attempt to generalise Munroe *et al.*'s (2012) approach, we present a spatially explicit
92 coupled demographic gene flow model that assesses the effect of demography variability on allele
93 frequencies in a marine metapopulation of sedentary benthic species with realistic population
94 densities. The seascape model was used to examine how: 1) demographic traits influence the
95 development of genetic structure in closed populations over time, 2) different patterns of
96 connectivity affect the loss or maintenance of genetic diversity in a metapopulation, 3) fluctuations
97 in local population density help maintain genetic diversity over time and 4) local population
98 stability impacts genetic diversity to provide relevant information for conservation decisions in the
99 Gulf of Lions, France.

100

101 **Methods**

102 *A seascape genetic model for benthic invertebrates with a pelagic larval phase*

103 To simulate the transient demographic effect on local allele frequencies arising from
104 environmental variability modulating connectivity through time, a seascape genetic model was
105 developed. The seascape model relies on the forcing of a spatially explicit dynamical model of
106 allele probability by a spatially explicit metapopulation model (Guizien *et al.*, 2014, adapted from
107 Hastings and Botsford 2006) (Fig. 1). The combination of these models allows us to project the
108 development of a population genetic structure through time, resulting from demography dynamics
109 driven by local survival and larval transfer on a regional scale.

110 The spatially explicit metapopulation model simulates the population density $N_i(t)$ at each
111 site i at any time t resulting from the balance of adult survival and input of new recruits resulting
112 from reproduction of adults present in the previous time step. Therefore, N_i represents the adult
113 census size per unit surface, and it is equal to the effective number of breeders per unit surface for
114 the next reproductive event (as defined by Waples *et al.*, 2013). It is important to note that such
115 formulation implicitly hypothesized that age at first reproduction and the time lapse between
116 reproductive events are both equal to the model time step, ensuring that effective number of
117 breeders does not vary with population age structure. Larval transfer rate among sites is estimated
118 from a set of realistic connectivity matrices obtained using the larval dispersal model (Guizien *et*
119 *al.*, 2012), and recruitment success (inter-specific competition or predation) is limited by saturating
120 population density (intra-specific competition) (Eq. 1 and 2) (Guizien *et al.*, 2014).

121

122
$$N_i(t+1) = \min(G(t) N_i(t), N_{max}) \quad (1)$$

123

124 $N_i(t+1)$ = Vector of spatial density of individuals at each site at time $t+1$ [individual per
125 m^2]

126 $N_i(t)$ = Vector of spatial density of individuals at each site at time t [individual per m²]

127 N_{max} = Saturating population density based on space limitation [individual per m²]

128

129 with the transfer matrix $G(t)$ defined by:

130

131
$$G_{ji}(t) = a_i C_{ji}(t) b_j + s_{jj} \delta_{ji} \quad (2)$$

132

133 a_i = Propagule production rate at site i [larvae per adult]

134 $C_{ji}(t)$ = Propagule transfer rate from site i to site j multiplied by the ratio of surface of site i
135 to surface of site j [no units]

136 b_j = Recruitment success at site j [adults per larva]

137 s_{jj} = Adult survivorship rate at site j [no units]

138 δ_{ji} = Kronecker symbol (1 when $i=j$, 0 otherwise)

139

140 Maximum population growth rate (P_i) of a closed population in site i is then defined by:

141
$$P_i = a_i b_i + s_{ii} \quad (3)$$

142

143 The time it takes for a population at any initial density N_o to reach its saturating density

144 N_{max} , from any given initial density was estimated as:

145

146
$$T = \frac{\ln\left(\frac{N_{max}}{N_o}\right)}{\ln(P_i)} \quad (4)$$

147

148 In the seascape genetics model, the frequency of each allele k is calculated at any given
 149 time in every site i , as a result of mixing between the surviving individuals with allele k in site i
 150 and the input of new recruits with allele k , coming from any other site (Eq. 5). Given the large
 151 number of larvae produced by each adult and the high larval survival values assigned (10%)
 152 compared to estimated regional retention rates (3%), genetic drift due to larval mortality is
 153 neglected and, thus, larval mortality is simulated as a proportional and uniform loss that is applied
 154 to the larval pool with allele k produced at each site. The effect of genetic drift is therefore
 155 simulated by the random sampling of the alleles lost during two different periods in the life cycle:
 156 larval dispersal and recruitment. Simplifying assumptions were that: 1) mating takes place
 157 randomly every year among diploid organisms, 2) allele frequencies are identical among sexes, 3)
 158 generations are discrete but overlapping, 4) populations are not age-structured, 5) given the
 159 relatively short period of time considered in the simulations (100 years), mutation is assumed to be
 160 negligible compared to genetic drift and migration, and thus set to zero and, 6) selection can be
 161 neglected.

162 During larval dispersal, the pool of larvae with allele k produced by each site, remaining in
 163 the region (accounting for regional retention rate), is randomly sampled before being re-distributed
 164 among the destination sites according to the connectivity matrix (Eq. 6 and 7). The number of
 165 larvae with allele k that will survive dispersal is computed by sorting out the rank of the allele
 166 carried by the surviving larvae. During recruitment, saturating density limits the number of
 167 arriving larvae that can be recruited at each site, therefore, a random subset of alleles carried by the
 168 pool of larvae arriving at each site is actually recruited.

169

170

$$p_{ik(t+1)} = \frac{(s_{ii} N_{i(t)} p_{ik(t)}) + b_j \sum_j \frac{C_{ij}}{\sum_l C_{lj} \frac{S_l}{S_j}} n'_{jk}{}^i}{N_{i(t+1)}} \quad (5)$$

171

172 where n'_{jk} is a random number between 0 and n_{jk} , with the constraint that $\sum_k n'_{jk} = n'_j$

173

174
$$n'_j{}^i = A_j a_j \left(\sum_l C_{lj} \frac{S_l}{S_j} \right) \quad (6)$$

175

176
$$n_{jk} = p_{jk} A_j a_j \quad (7)$$

177

178 $p_{ik(t+1)}$ = Frequency of allele k at site i at time $t+1$ [no units]

179 $p_{ik(t)}$ = Frequency of allele k at site i at time t [no units]

180 $p_{jk}(t)$ = Frequency of allele k at site j at time t [no units]

181 S_i = Surface area of site i [m²]

182 A_j = Density of individuals in site j [individual per m²]

183 $n'_{jk}{}^i$ = Number of larvae produced per unit surface in site j having allele k that remain in

184 the region and will survive until sexual maturity in site i

185 $n'_j{}^i$ = Number of larvae produced per unit surface in site j that remain in the region and

186 survive until sexual maturity in site i

187 n_{jk} = Number of larvae with allele k produced in site j per unit surface

188

189 *Test cases*

190 The simulations were designed to evaluate the changes in allele frequencies due to

191 variations in species demographic parameters and connectivity structure. Although this modelling

192 approach applies to any sedentary species with a reproductive dispersive stage, to test the

193 sensitivity of the model, we focused on marine benthic species with four different life expectancies
194 (2, 5, 10 and 20 years) that reproduce each year. The values of minimum recruitment success were
195 varied in order to test the effect of maximum population growth in the maintenance of genetic
196 diversity over time. Minimum recruitment success was also the same in all populations (10%),
197 although it was limited by saturating spatial density, which was set to $N_{max}=6250$ individuals/m²
198 per population.

199 Six groups of simulations were performed (Table 1). All simulations were run for 100
200 iterations, one iteration being the time lapse between two reproductive events. The initial genetic
201 structure was described by ten different alleles present simultaneously in every site. In order to
202 remove the potential bias due a specific initial condition for the genetic structure, simulations were
203 repeated at least 100 times with different and random initial conditions of allele frequencies.

204 The first group consisted of simulations of a closed population (no larval inputs) in which
205 life expectancy was raised from two to 20 years. Groups 2, 3A, 3B, 4A and 4B, consisted of
206 simulations of a metapopulation of a species with a life expectancy of 10 years, distributed among
207 32 sites along the Gulf of Lions (northwestern Mediterranean) (Fig. 2), in which spatial structure
208 was driven by connectivity only. These groups of simulations correspond to the test case of
209 dominating species of the soft-bottom benthic communities in the Gulf of Lions (polychaetes). The
210 continuous sandy-bottom habitat was described by sites of approximately the same width (~ 20
211 km) contiguously distributed along the coast spanning the 10 to 30 meters isobaths. Based on these
212 criteria, the areas of the 32 sites ranged from 6.2 to 121 km². Survival and fecundity rates were the
213 same among populations within the metapopulation and were kept constant over time in all of the
214 simulations.

215 Larval transfer between the 32 sites was computed from Lagrangian larval dispersal
216 simulations based on regional hydrodynamic simulations performed with the coastal circulation
217 model SYMPHONIE (Marsaleix *et al.*, 2008). Larval dispersal was simulated by releasing larvae

218 at the average site depth (20 m). Connectivity matrices containing larval transfer probabilities were
219 produced for 20 sets of 10-day long spawning periods in 2004 and 2006 with an average PLD of
220 four weeks (Guizien *et al.*, 2014). A total of 20 different connectivity matrices were used for this
221 analysis.

222 Simulations of Group 2 were performed to evaluate the effect of the distinct connectivity
223 structure on heterozygosity. In this case, connectivity was set deterministically using the same
224 connectivity matrix every year (either one of the 20 variants) and, thus, simulations were only run
225 100 times.

226 Groups 3A, 3B, 4A and 4B were performed in order to test the effect of recruitment (3A
227 and 3B) and habitat loss (4A and 4B) on metapopulation size and the maintenance of
228 heterozygosity within a metapopulation over time. Metapopulation size was represented as average
229 regional coverage, defined as the ratio between regional average population density and saturating
230 density. Connectivity was set stochastically using a different connectivity matrix among the 20
231 variants every year and, thus, simulations were run 500 times to reach the convergence of the mean
232 when combining stochasticity in connectivity and initial condition. Group 3A simulated gene flow
233 among all populations, and recruitment success was constant every year. Group 3B explored a
234 scenario where recruitment failure (no recruitment) occurred every three years. Group 4A
235 simulated the loss of four populations (sites 17, 18, 19 and 20). These populations were identified
236 as being essential for the regional persistence of species at minimum recruitment success in
237 metapopulation modelling, comparing the vulnerability to habitat loss of four ports in the Gulf of
238 Lions (Guizien *et al.*, 2014). Nonetheless, it is important to mention that for the present
239 simulations, the values of minimum recruitment success and fecundity were set to ensure long-
240 term persistence of the metapopulation after removing those four sites, unlike in Guizien *et al.*
241 (2014). Group 4B evaluated a scenario where only one population (site 21) was lost from the
242 metapopulation. This site was characterised by consistently showing the highest values of

243 betweenness in the metapopulation when applying graph theory analysis to connectivity matrices
 244 (Costa, *pers. comm.*).

245

246 *Metrics and statistics*

247 Heterozygosity and allelic richness are two measures of genetic diversity commonly used
 248 in the population genetics literature, and in the present study both were used. Heterozygosity (H_e),
 249 was estimated taking into account all individuals at each site i over time (Eq. 7).

250

251
$$H_e(t) = \frac{1}{n} \sum_{k=1}^n p_{ik}(t)^2 \quad (7)$$

252

253 where $p_{ik}(t)$ = frequency of the k th allele of n alleles in site i at time t [no units].

254

255 However, heterozygosity and allelic richness describe the state of genetic diversity of a
 256 population at a particular time and not its dynamics. In order to measure the speed at which genetic
 257 diversity varied as a function of demographic parameters (regulating genetic drift) and
 258 connectivity structure, new metrics describing the initial and average slope of the evolution of
 259 genetic diversity over time are introduced: 1) Allele Drifting Time (T_d), which is the moment at
 260 which allelic diversity starts decreasing, meaning the time when the first allele is lost from the
 261 population or the metapopulation. 2) Allele Fixation Time (T_f), which is the time lapse between
 262 the first loss of an allele (T_d) and the fixation of any allele (Fig. 3).

263 These metrics were defined on allelic richness rather than heterozygosity to avoid
 264 ambiguity in defining genetic diversity reference points and given the known sensitivity of allelic
 265 richness to the loss of rare alleles (Allendorf 1986).

266
$$A_e(t) = \frac{1}{n} \sum_{k=1}^n p_{ik}(t)$$

267 **Results**

268 *Do differences in demographic parameters affect genetic diversity in closed populations?*

269 Figures 4A and 4B display the loss of genetic diversity in closed populations at initial
270 saturating capacity as a function of the ratio between mortality (being complementary to unity of
271 survival) and recruitment success. This ratio, having the dimensions of larvae/adult/year, depicts
272 the origin of recruitment regulation (*sensu* by Hixon *et al.*, 2002) and informs on the relative
273 contribution of intrinsic vs. extrinsic drivers: high values indicate recruitment regulation due to
274 low recruitment success driven by inter-specific competition or predation, while low ratio values
275 indicate recruitment regulation due to space limitation at a high population density (intra-specific
276 competition). The observed relationship between the loss of genetic diversity (measured as T_d) and
277 recruitment success in these simulations, as it is defined in Equation 2, also reflects the
278 relationship between T_d and local retention in the case of an isolated population.

279 Fig. 4A shows that the number of reproductive events after which the population begins to
280 loose its genetic diversity (T_d/Re) increases with the ratio between mortality and recruitment
281 success. This demonstrates a reduction of genetic drift when recruitment success decreases for any
282 given life expectancy. However, genetic drift is inhibited at high levels of recruitment success, as
283 depicted by low and almost constant T_d/Re for the lowest values of the ratio between mortality and
284 recruitment success. Such minimum T_d/Re is of the order of magnitude of the number of
285 reproductive events in a life expectancy. For a recruitment frequency of 0.18, short-lived species
286 (two years) could start loosing their genetic diversity after three years, while it would take around
287 14 years for a long-lived species (20 years). This reflects the effect of genetic drift inhibition by
288 the reduction of reproductive events due to the lack of space caused by the presence of adults as
289 life expectancy increases.

290 Similarly, the maintenance of genetic diversity, measured by the number of reproductive
291 events before allele fixation (T_f/Re), in closed populations at an initial saturating density increases

292 with life expectancy, regardless of whether the population growth rate is low (<2.5) or high (>2.5)
293 (Fig. 5). This confirms that genetic drift is limited by population inertia due to recruitment
294 inhibition as a result of space limitation, as neither fecundity nor recruitment success affects the
295 relationship.

296 However, when dealing with overlapping generations, it must be taken into account that
297 the reduction of genetic drift by space limitation during the first population turnover decreases
298 with species longevity. This is exhibited by the different hierarchies between life expectancy
299 curves when representing the time at which the population starts to lose its genetic diversity in
300 terms of population turnover (adimensionalising T_d by the life expectancy of the species) (Fig.
301 4B). Species with short life expectancies begin to experience a reduction of their genetic diversity
302 after a higher number of population turnovers than do long-lived species, as fewer reproductive
303 events occur during a short life expectancy compared to during a long one. This result confirms
304 that genetic drift can be controlled by effective reproduction (which may be limited by long life
305 expectancy or low recruitment success) and its frequency along the species lifespan in a context of
306 finite population size.

307 Different initial population densities also affect the time at which a population starts
308 losing genetic diversity (Fig. 6A) – for any value of the ratio between mortality and recruitment
309 success, the lower the initial density of the population, the slower the loss of genetic diversity. This
310 result points out that genetic drift is slower when considerable space is available for recruitment
311 compared to at saturating density where space availability is regulated by mortality. Quantifying
312 space availability by the time it will take a population to reach saturating density (6250
313 individuals/m²) shows that it would take twice as long for a population with an initial density of 50
314 individuals/m² compared to a population with an initial density of 1000 individuals/m² (Fig. 6B).
315 Allele drifting time increases linearly with the time necessary to reach saturating density.

316 The population growth rate triggers the effect of initial population density when it comes

317 to the maintenance of genetic diversity, measured as T_f (Fig. 5). While in fast growing
318 populations, the maintenance of genetic diversity is not sensitive to initial density, in slow growing
319 populations, the maintenance of genetic diversity lasts longer and is more variable when the initial
320 population size is small (50 individuals/m²) compared to when it is at saturating density. Such
321 sensitivity to initial population size is amplified at small life expectancies.

322 Overall, in closed populations, genetic drift is the quickest when the population is at
323 saturating density with high recruitment success, slowing down at low recruitment success or when
324 population size is lower than saturating density. This result demonstrates the importance of
325 transient demography in regulating the speed of genetic drift.

326

327 *Do different patterns of connectivity affect the maintenance of genetic diversity in a*
328 *metapopulation?*

329 Simulated heterozygosity patterns among populations forming a metapopulation varied
330 according to each connectivity matrix. The two most contrasting spatial patterns with low
331 heterozygosity values either in the west (A) or in the east (B) of the Gulf of Lions are shown in
332 Fig. 7. A plausible explanation is the different spatial patterns of local retention (defined as the
333 proportion of larvae produced locally that remain in the same spatial unit) vs. import (estimated as
334 the proportion of all larvae produced among all sites that settled within the focal site). For
335 connectivity matrix 1, the ratio between local retention and import was higher in the west than in
336 the east (0.074 and 0.027, respectively). On the contrary, for connectivity matrix 2 the values of
337 the same ratio were higher in the east compared to the west (0.069 and 0.0085, respectively).
338 However, simulations demonstrated that the relationship between T_d and import do not exhibit any
339 trend with no linear correlation ($R^2 = 0.011$; $P < 0.01$) (Figure S1). Similarly, T_d was not linearly
340 correlated to local retention rate values obtained from the analysis of the 20 connectivity matrices
341 ($R^2 = 0.031$; $P > 0.05$). However, T_d was delimited by a piecewise function enabling the

342 discrimination between two groups (Fig. 8) – populations with low levels of local retention (< 2%)
343 that show high variability in the time they begin to lose their genetic diversity (Td/Le ranging
344 from 0.2 to 50) and populations with high local retention (> 2%) where genetic drift is much
345 quicker and less variable (Td/Le ranging from 0.2 to 12). This indicates that the speed of genetic
346 drift is regulated locally only at a high local retention rate (larger than 2%) while, for local
347 retention rates lower than 2%, the strength of genetic drift depends on the regional structure of
348 connectivity. According to the direction of the transfer and the genetic characterisation of the
349 contributing populations, genetic drift will then be accelerated or slowed down in the focal
350 population.

351

352 *How does local population stability affect heterozygosity in a metapopulation?*

353 When looking into the variation of the average heterozygosity in the metapopulation
354 through time for a species with a life expectancy of 10 years, it becomes clear that changes in
355 population density have a major effect on the loss of genetic diversity in a metapopulation (Fig. 9).
356 The rate at which a metapopulation reaches a stable regional coverage influences its possibility to
357 maintain genetic diversity over time, even in the presence of migration.

358 Overall, we observe that as soon as regional coverage reaches 80%, heterozygosity
359 values decrease rapidly and genetic diversity is lost. Scenario A shows how, with constant
360 recruitment success, the effect of migration among populations homogenises allele frequencies
361 over time and leads to the fixation of the same allele in all populations over a relatively short
362 period of time. Most interestingly, in Scenario B, we find that high variability in metapopulation
363 regional coverage due to recurrent failures in recruitment actually helps maintain genetic diversity
364 over time. Stochastic connectivity leading to demographical fluctuations in populations enables the
365 maintenance of genetic diversity.

366 On the other hand, Scenario C exemplifies how, in the Gulf of Lions, removing

367 populations (sites 17–20) responsible for bringing demographic persistence to the metapopulation
368 at minimum recruitment success divides it into an eastern and western group, causing a slightly
369 faster decrease of genetic diversity in the latter group than in the former. However, Scenario D
370 shows how the loss of only one site, identified as essential for maintaining the integrity of the
371 connectivity graph, indeed disrupts the genetic connectivity of the metapopulation by augmenting
372 the differentiation between the eastern and western groups in terms of the loss of heterozygosity,
373 with drifting starting earlier in the eastern part. In Scenarios C and B, recruitment success was set
374 in order to ensure that the loss of sites within the metapopulation would still allow for species
375 persistence. It should be noticed that in both scenarios, a similar constant metapopulation size was
376 maintained, even if not at saturating density. The effect of migration in this case will also lead to
377 the loss of genetic diversity in the metapopulation over time, although at a slower rate.

378

379 **Discussion**

380 The present study highlights that genetic drift increases considerably with settlement and
381 post-settlement limitations due to space availability when the effective number of breeders is
382 approaches saturating capacity, and causes a strong reduction of effective population size.

383 Early authors had already shown how changes in genetic diversity are related to effective
384 population size (Wright 1931; Kimura 1955). Nonetheless, it has been demonstrated theoretically
385 that life cycle processes, like overlapping generations (Jorde and Ryman 1995), and demographic
386 parameters can also have an effect on the amount of temporal allele frequency change and should
387 be taken into account (Ryman 1997). Our results highlight the role of life cycle processes, other
388 than age at first reproduction (Lee *et al.*, 2011), in reducing effective population size and
389 increasing the effect of genetic drift. In closed populations, recruitment intensity regulates the
390 speed of genetic drift on genetic diversity, demonstrating the relevance of transient demography in
391 shaping the genetic structuration of marine species. In open populations, genetic drift is slowed

392 down as a result of larval exchange. The effect of recruitment failure and the loss of key source
393 populations on heterozygosity confirm that transient demographic fluctuations, remaining above
394 the risk of regional extirpation, actually help maintain genetic diversity over time.

395 Recently, several meta-analyses and empirical studies evaluating the relationship between
396 PLD and population genetic differentiation across different marine species indicated a weak
397 correlation between the two (Selkoe and Toonen 2011; Faurby and Barber 2012). In some cases,
398 the high uncertainty in the estimates of larval dispersal and measures of population differentiation
399 were suggested as the main causes for the unexpected results, while other studies suggested that
400 differential mortalities and levels of abundance among populations were more relevant (Munroe *et*
401 *al.*, 2012). The results from our simulations support these findings, while further demonstrating
402 that considering other biological parameters and the inclusion of transient dynamics caused by
403 other demographic parameters, such as life expectancy, fecundity, local retention and recruitment
404 success, would help explain better the variability of genetic connectivity in a metapopulation.

405 Dawson *et al.* (2014), found that differences in fecundity, population size and PLD could
406 account for the differences in population genetic structure between eight co-distributed rocky
407 intertidal invertebrate species in the eastern North Pacific. They found that population size was
408 positively related to population genetic structure and they attributed the variability among species
409 to differences in recruitment and demography. Furthermore, they highlighted that the differences
410 in migration potential found between theoretical and empirical data could be attributed to the role
411 of genetic drift and natural selection. Here, we corroborate their hypotheses by demonstrating how
412 the strength of genetic drift is influenced by recruitment success, local retention and fluctuations in
413 population density due to habitat fragmentation and recruitment.

414 Our results confirm that genetic drift is controlled by effective reproduction, as it is
415 observed when genetic diversity decreases due to a reduction of recruitment success caused by
416 space limitation, rather than changes in the number of reproductive adults in the population. This is

417 particularly the case when the filtering during reproduction applies to the fate of the larvae and not
418 on the adults contributing to reproduction. We demonstrate that a long life expectancy and low
419 recruitment success regulate the temporal variation of allele frequencies and reduce the loss of
420 genetic diversity over time. This provides an alternative explanation to empirical evidence of
421 strong genetic structure in long-lived species, when recruitment success is limited by space
422 availability. In fact, it has already been shown how a long-lived species, such as the red coral
423 *Corallium rubrum*, can exhibit patterns of strong genetic differentiation at small spatial scales (tens
424 of metres) in the Mediterranean Sea, suggesting that this could result from recruitment regulation
425 by low population turnover (Costantini *et al.*, 2007).

426 Population regulation occurs when at least one demographic rate is density-dependent
427 (Hixon *et al.*, 2002). Clear evidence of genetic drift accelerating due to recruitment regulation is
428 observed in our simulations for closed populations at the initial saturating density. Furthermore,
429 the evaluation of the ratio between mortality and recruitment success allowed for disentangling the
430 relative contribution of intrinsic (intra-specific competition) vs. extrinsic drivers (inter-specific
431 competition or predation).

432 In open systems, it was already suggested that the amount of local retention could have a
433 strong influence on the relative importance of demographic vs. connectivity parameters in the
434 dynamics of metapopulations (Figueira 2009). Our results confirm those findings and indicate that
435 local retention rate values larger than 2% diminish the influence of the connectivity structure over
436 genetic drift, as genetic drift accelerates in those populations close to saturating capacity. This is
437 particularly relevant for the spatial planning of MPAs. Whether an MPA is created for the
438 conservation of biodiversity or for fishery management, its main purpose is to maintain the
439 persistence of its populations. In the case of marine metapopulations, local retention is considered
440 the currency of persistence: the higher the local retention, the closer the population is to its
441 saturating capacity (Burgess *et al.*, 2014). Nonetheless, it is important to note that, as Figueira

442 (2009) suggested, under the same flow structure, differences in PLD among species could cause
443 distinct patterns of local retention for different species in the same place, making biodiversity
444 conservation efforts even more difficult. In any case, the loss of genetic variability through genetic
445 drift at a high local retention rate can diminish future adaptability to a changing environment,
446 which might be detrimental to local conservation efforts, strongly advocating for a network of
447 MPAs formed by sites with lower local retention rate.

448 The maintenance of genetic diversity in the metapopulation over at least 100 years in the
449 case of regular recruitment failure, creating regional demographic fluctuations, was not
450 unexpected. These results, incorporating realistic spatially explicit connectivity matrices, extend
451 previous theoretical studies that found that demographic instability and fluctuations in migration
452 produce major changes in the evolution of genetic variation and population differentiation
453 (Whitlock 1992). Demographic disturbances due to population bottlenecks have been shown to
454 induce strong genetic drift. In the present study, demographic disturbances around saturating
455 capacity can reversely reduce the effect of genetic drift. Furthermore, our results suggests that
456 there is a potential for opposing effects to population disturbances depending on the condition of
457 the population prior to the disturbance: 1) accelerating genetic drift when population census size is
458 high with recruitment limitation, or 2) decelerating genetic drift when population census size is
459 low with no recruitment limitation.

460 Given that disturbances can cause variations in key demographic and biological
461 processes, disturbance history may be one of the major drivers shaping the patterns of genetic
462 diversity in many natural populations (Banks *et al.*, 2013). The pattern of genetic diversity
463 maintenance over time observed in our simulations has been reported in an empirical study on
464 natural populations of frogs, where no losses of genetic diversity after a disturbance were found
465 when survival was high or when recovering populations recruited many individuals from multiple
466 sources (Spear *et al.*, 2012). In addition, Larson *et al.* (1984) suggested, based on a survey of 22

467 species of salamanders, that historical influences are much more important in describing genetic
468 variation patterns than is recent migration.

469 Previous studies in the region identified the spatial structuration of population
470 vulnerability to habitat loss driven by hydrodynamical connectivity. Four sites essential for species
471 regional persistence at minimum recruitment success were identified from metapopulation
472 modelling around the port of Sète (sites 17–20, Guizien *et al.*, 2014). However, analysis of the
473 same connectivity graph used in the metapopulation model depicted those four sites as high
474 bridging centrality, spanning across the two subclusters of the region. Another site (site 21) was
475 instead identified for maintaining network integrity, as depicted by the highest betweenness (Costa,
476 *pers. comm*). Here, we show that both the loss of four essential populations and the loss of the
477 highest betweenness site divide the metapopulation into two genetically distinct subpopulations
478 (eastern and western). Nevertheless, the loss of only site 21 leads to a higher level of genetic
479 differentiation in the metapopulation. This result suggests that the highest betweenness of
480 hydrodynamical connectivity graph could be interpreted for relaying gene flow and maintaining
481 genetic connectivity, similar to how Rozenfeld *et al.* (2008) interpreted the highest betweenness of
482 genetic distance. This example encourages further investigation of the potential of graph analysis
483 of hydrodynamical connectivity matrices to identify sites important for conservation of genetic
484 diversity.

485 On a local scale, high local retention, which helps maintain a species in isolated protected
486 marine areas, accelerates genetic drift and as a result, accelerates the reduction of genetic diversity.
487 At the network level, the site having the most important role in heterozygosity maintenance
488 (highest betweenness) did not correspond to those sites identified as essential for regional
489 persistence in the metapopulation. The combination of these findings poses a question for
490 management: in order to protect species persistence and genetic diversity, should we be seeking a
491 compromise between preserving populations that are low in terms of diversity but are also

492 demographically stable vs. highly diverse but unstable populations? The present model, by
493 combining demography and gene flow in realistic conditions allows to 1) disentangle the relative
494 contribution of local demography and environmental connectivity in shaping seascape genetics,
495 and 2) perform *in silico* evaluations of different scenarios for marine spatial planning.

496

497 **Acknowledgments**

498 This work was (co-)funded through a MARES Grant. MARES is a Joint Doctorate programme se-
499 lected under Erasmus Mundus coordinated by Ghent University (FPA 2011-0016). Check
500 www.mares-eu.org for extra information. This work was also partly funded by the French National
501 Program LITEAU IV of the Ministère de l'Écologie et de l'Environnement Durable under project
502 RocConnect—Connectivité des habitats rocheux fragmentés du Golfe du Lion (PI, K. Guizien,
503 Project Number 12-MUTS-LITEAU-1-CDS-013). We would like to thank Proof-reading-
504 service.com for English edition and corrections of the manuscript, and Dr. Lorenzo Bramanti for
505 an early critical review of the manuscript.

506

507 **References**

- 508 Aiken, C., and Navarrete, S. 2011. Environmental fluctuations and asymmetrical dispersal:
509 Generalized stability theory for studying metapopulation persistence and marine protected
510 areas. *Marine Ecology Progress Series*, 428: 77–88.
- 511 Alcalá, N., Streit, D., Goudet, J., and Vuilleumier, S. 2013. Peak and persistent excess of genetic
512 diversity following an abrupt migration increase. *Genetics*, 193: 953–971.
- 513 Banks, S. C., Cary, G. J., Smith, A. L., Davies, I. D., Driscoll, D. A., Gill, A. M., Lindenmayer, D.
514 B., *et al.* 2013. How does ecological disturbance influence genetic diversity? *Trends in*
515 *Ecology & Evolution*, 28: 670–679.
- 516 Botsford, L., White, J., Coffroth, M., Paris, C., Planes, S., Shearer, T., Thorrold, S., *et al.* 2009.

517 Connectivity and resilience of coral reef metapopulations in marine protected areas: Matching
518 empirical efforts to predictive needs. *Coral Reefs*, 28: 327–337.

519 Burgess, S., Nickols, K., Griesemer, C., Barnett, L., Dedrick, A., Satterthwaite, E., Yamane, L., *et*
520 *al.* 2014. Beyond connectivity: How empirical methods can quantify population persistence to
521 improve marine protected-area design. *Ecological Applications*, 24: 257–270.

522 Costantini, F., Fauvelot, C., and Abbiati, M. 2007. Genetic structuring of the temperate gorgonian
523 coral (*Corallium rubrum*) across the western Mediterranean Sea revealed by microsatellites
524 and nuclear sequences. *Molecular Ecology*, 16: 5168–5182.

525 Cowen, R., and Sponaugle, S. 2009. Larval dispersal and marine population connectivity. *Annual*
526 *Review of Marine Science*, 1: 443–466.

527 Dawson, M., Hays, C., Grosberg, R., and Raimondi, P. 2014. Dispersal potential and population
528 genetic structure in the marine intertidal of the eastern North Pacific. *Ecological Monographs*,
529 84: 435–456.

530 Faurby, S., and Barber, P. 2012. Theoretical limits to the correlation between pelagic larval
531 duration and population genetic structure. *Molecular Ecology*, 21: 3419–3432.

532 Figueira, W. 2009. Connectivity or demography: Defining sources and sinks in coral reef fish
533 metapopulations. *Ecological Modelling*, 220: 1126–1137.

534 Galindo, H., Olson, D., and Palumbi, S. 2006. Seascape genetics: A coupled oceanographic-
535 genetic model predicts population structure of Caribbean corals. *Current Biology*, 1622–1626.

536 Gilg, M., and Hilbish, T. 2003. The geography of marine larval dispersal-coupling genetics with
537 fine-scale physical oceanography. *Ecology*, 1–11.

538 Guizien, K., Belharet, M., Marsaleix, P., and Guarini, J. M. 2012. Using larval dispersal
539 simulations for marine protected area design: Application to the Gulf of Lions (northwest
540 Mediterranean). *Limnology and Oceanography*, 57: 1099–1112.

541 Guizien, K., Belharet, M., Moritz, C., and Guarini, J. M. 2014. Vulnerability of marine benthic

542 metapopulations: Implications of spatially structured connectivity for conservation practice in
543 the Gulf of Lions (NW Mediterranean Sea). *Diversity and Distributions*, 1–11.

544 Guizien, K., Brochier, T., Duchêne, J. C., Koh, B. S., and Marsaleix, P. 2006. Dispersal of *Owenia*
545 *fusiformis* larvae by wind-driven currents: Turbulence, swimming behaviour and mortality in
546 a three-dimensional stochastic model. *Marine Ecology Progress Series*, 311: 47–66.

547 Hastings, A., and Botsford, L. 2006. Persistence of spatial populations depends on returning home.
548 *Proceedings of the National Academy of Sciences*, 103: 6067–6072.

549 Hastings, A., and Harrison, S. 1994. Metapopulation dynamics and genetics. *Annual Review of*
550 *Ecology, Evolution, and Systematics*, 25: 167–188.

551 Hellberg, M. 1996. Dependence of gene flow on geographic distance in two solitary corals with
552 different larval dispersal capabilities. *Evolution*, 50: 1167–1175.

553 Hellberg, M., Burton, R., Neigel, J., and Palumbi, S. 2002. Genetic assessment of connectivity
554 among marine populations. *Bulletin of Marine Science*, 70: 273–290.

555 Hixon, M., Pacala, S., and Sandin, S. 2002. Population regulation: Historical context and
556 contemporary challenges of open vs. closed systems. *Ecology*, 83: 1490–1508.

557 Jorde, P., and Ryman, N. 1995. Temporal allele frequency change and estimation of effective size
558 in populations with overlapping generations. *Genetics*, 139: 1077–1090.

559 Kimura, M. 1955. Random genetic drift in multi-allelic locus. *Evolution*, 9: 419–435.

560 Kool, J. 2009. An object-oriented, individual-based approach for simulating the dynamics of genes
561 in subdivided populations. *Ecological Informatics*, 4: 136–146.

562 Larson, A., Wake, D., and Yanev, K. 1984. Measuring gene flow among populations having high
563 levels of genetic fragmentation. *Genetics*, 106: 293–308.

564 Lee, A., Engen, S., and Saether, B. 2011. The influence of persistent individual differences and age
565 at maturity on effective population size. *Proceedings of the Royal Society B: Biological Sci-*
566 *ences*, 278: 3303–3312.

567 Lowe, W., and Allendorf, F. 2010. What can genetics tell us about population connectivity?
568 *Molecular Ecology*, 19: 3038–3051.

569 Marko, P., and Hart, M. 2011. The complex analytical landscape of gene flow inference. *Trends in*
570 *Ecology & Evolution*, 26: 448–456.

571 Marsaleix, P., Auclair, F., Floor, J., Herrmann, M., Estournel, C., Pairaud, I., and Ulses, C. 2008.
572 Energy conservation issues in sigma-coordinate free-surface ocean models. *Ocean Modelling*,
573 20: 61–89.

574 Munroe, D., Klinck, J., Hofman, E., and Powell, E. 2012. The role of larval dispersal in
575 metapopulation gene flow: Local population dynamics matter. *Journal of Marine Research*, 1–
576 2441–4677.

577 Palumbi, S. 2004. Marine reserves and ocean neighborhoods: The spatial scale of marine
578 populations and their management. *Annual Review of Environment and Resources*, 29: 31–
579 68.

580 Pineda, J. 2000. Linking larval settlement to larval transport: assumptions, potentials and pitfalls.
581 *Oceanography of the Eastern Pacific*, 84–105.

582 Pineda, J., Hare, J., and Sponaugle, S. 2007. Larval transport and dispersal in the coastal ocean and
583 consequences for population connectivity. *Oceanography*, 20: 22–39.

584 Riginos, C., Douglas, K., Jin, Y., Shanahan, D., and Treml, E. 2011. Effects of geography and life
585 history traits on genetic differentiation in benthic marine fishes. *Ecography*, 34: 566–575.

586 Rozenfeld, A., Arnaud-Haond, S., Hernández-García, E., Eguíluz, V., Serrão, E., and Duarte, C.
587 2008. Network analysis identifies weak and strong links in a metapopulation system.
588 *Proceedings of the National Academy of Sciences*, 105: 18824–18829.

589 Ryman, N. 1997. Minimizing adverse effects of fish culture: Understanding the genetics of
590 populations with overlapping generations. *ICES Journal of Marine Science*, 54: 1149–1159.

591 Saenz-Agudelo, P., Jones, G., Thorrold, S., and Planes, S. 2009. Estimating connectivity in marine

592 populations: an empirical evaluation of assignment tests and parentage analysis under
593 different gene flow scenarios. *Molecular Ecology*, 18: 1765–1776.

594 Selkoe, K., and Toonen, R. 2011. Marine connectivity: A new look at pelagic larval duration and
595 genetic metrics of dispersal. *Marine Ecology Progress Series*, 436: 291–305.

596 Siegel, D., Kinlan, B., Gaylord, B., and Gaines, S. 2003. Lagrangian descriptions of marine larval
597 dispersion. *Marine Ecology Progress Series*, 260: 83–96.

598 Spear, S., Crisafulli, C., and Storfer, A. 2012. Genetic structure among coastal tailed frog
599 populations at Mount St. Helens is moderated by post-disturbance management. *Ecological*
600 *Applications*, 22: 856–869.

601 Waples, R., Luikart, G., Faulkner, J., and Tallmon, D. 2013. Simple life-history traits explain key
602 effective population size ratios across diverse taxa. *Proceedings of the Royal Society B: Bio-*
603 *logical Sciences*, 280: 20131339.

604 Werner, F., Cowen, R., and Paris, C. 2007. Coupled biological and physical models.
605 *Oceanography*, 1–16.

606 Whitlock, M. 1992. Temporal fluctuations in demographic parameters and the genetic variance
607 among populations. *Evolution*, 46: 608–615.

608 Wright, S. 1931. Evolution in Mendelian populations. *Genetics*, 16: 97–159.

609

610 **Table 1.** Settings of six simulation groups. Connectivity, when present, was set either
611 deterministically (D) using the same matrix every year (either one of the 20 variants) or
612 stochastically (S) picking a different matrix among the 20 variants every year. Disturbance
613 scenarios were only applied to the groups with stochastic connectivity.
614

614

	Group 1	Group 2	Group 3A	Group 3B	Group 4A	Group 4B
Connectivity	NO	D	S	S	S	S
Initial population density (Individuals/m²)	50, 1000, Nmax	50	50	50	50	50
Fecundity	1000	2000	2000	2000	2000	2000
Life expectancy	2,5,10 and 20 years	5 years	10 years	10 years	10 years	10 years
Number of simulations	100	100	500	500	500	500
Disturbance	NO	NO	NO	Recruitment failure	Habitat loss (source sites)	Habitat loss (betweenness)

615

616

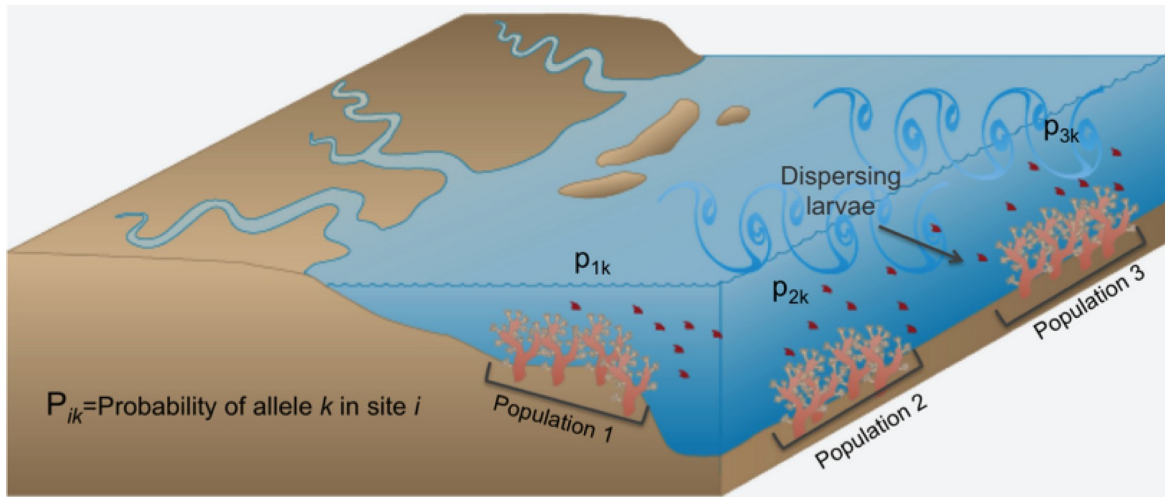
617

618

619

620

621



623

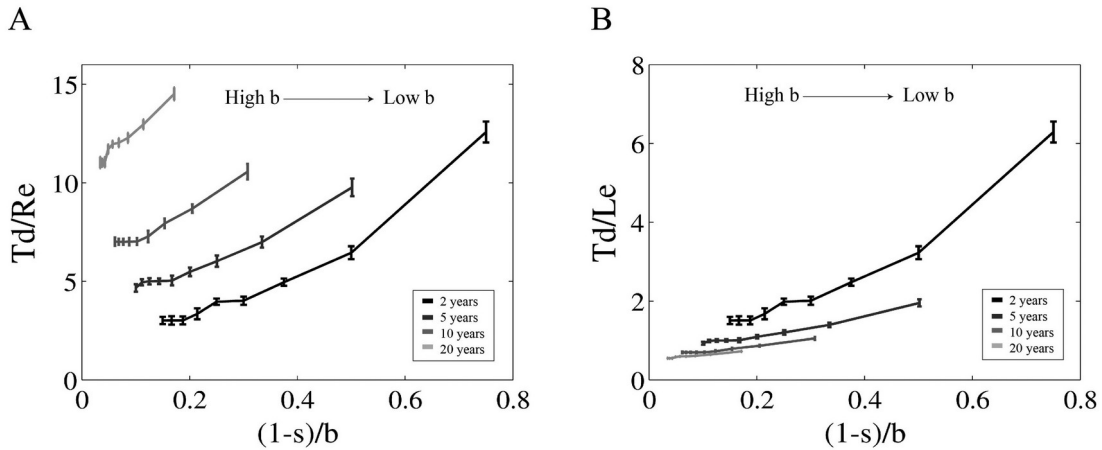
624 **Figure 1.** Schematic representation of seascape genetic model. The frequency of each
625 allele k is calculated at any given time in every site i , as a result of mixing between the
626 surviving individuals with allele k in site i and to the input of new recruits with allele k ,
627 coming from any other site.

628

629

630

631



633
 634 **Figure 2.** Effect of different life expectancies on the loss of genetic diversity, measure as
 635 allele drifting time (T_d), for an isolated population at initial saturating capacity (6250 ind.
 636 m^{-2}). Adimensionalizing allele drifting time by the number of reproductive events (T_d/Re) (a) represents the differences in the number of generations it takes for a species
 637 with different life expectancies to start losing its genetic diversity as a function of the
 638 ratio between mortality and recruitment success. In contrast, adimensionalizing allele
 639 drifting time by the life expectancy (T_d/Le) of a species (b) provides a different vision
 640 corresponding to population turnover.
 641

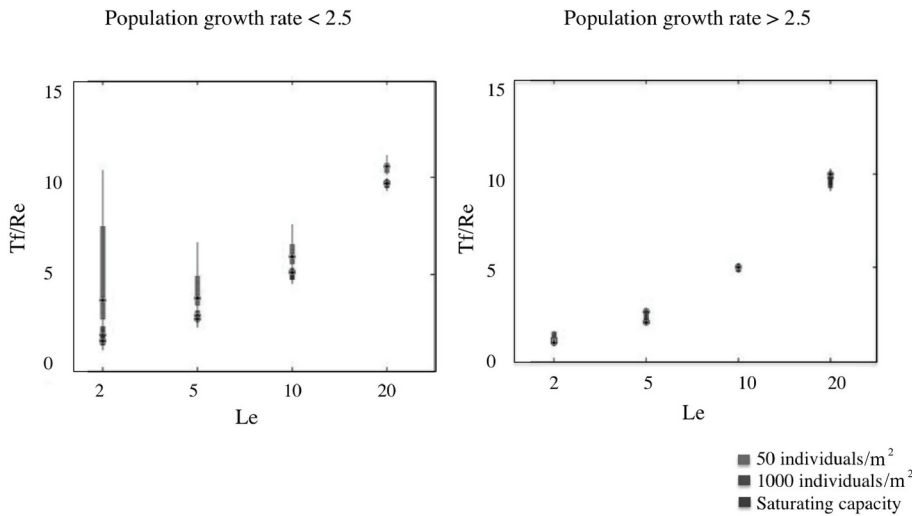
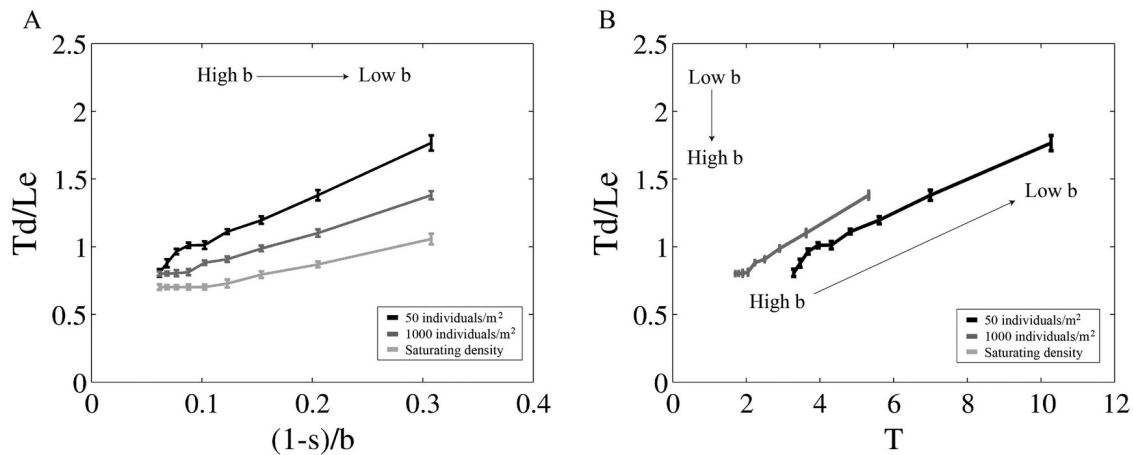


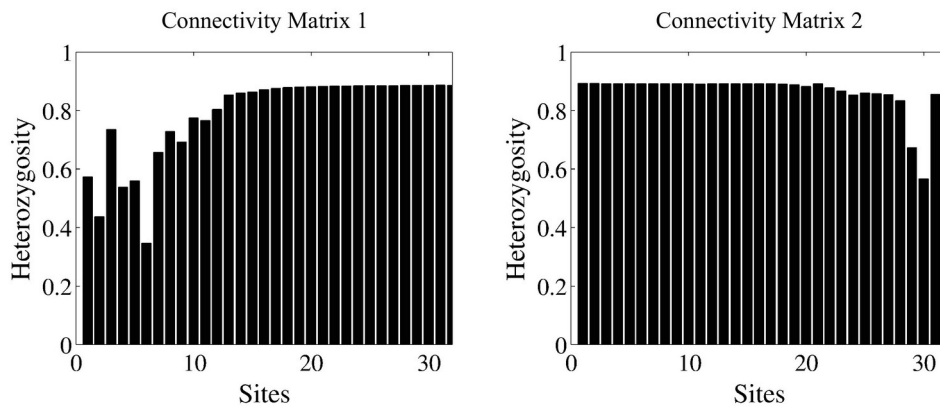
Figure 3.

661 Effect of population growth rate over allele fixation time (T_f) for three different initial
 662 conditions of population abundance (50, 1000, and 6250 ind. m^{-2}) as a function of species
 663 life expectancy (Le) in a closed population.
 664
 665



667
 668 **Figure 4.** Effect of different initial population abundances (50, 1000, and 6250 ind. m⁻²)
 669 on the loss of genetic diversity, measured as allele drifting time ($T d$), as a function of (a)
 670 the ratio between mortality and recruitment success $[(1-s)/b]$, and (b) the time to reach
 671 saturating capacity (T). $T d$ is adimensionalized by the life expectancy ($T d /Le$) of a
 672 species that lives 10 years, thus representing the number of population turnovers to start
 673 losing genetic diversity in an isolated population.

674
 675
 676
 677
 678
 679
 680
 681
 682
 683
 684
 685
 686
 687
 688



689 **Figure 5.** Spatial pattern of genetic diversity caused by distinct connectivity structures.
 690 Variability of heterozygosity for 32 sites forming a metapopulation for a species with a
 691 life expectancy of 5 years.

692
 693
 694
 695
 696
 697
 698

699
700
701
702
703
704
705
706
707
708
709
710
711
712
713
714
715
716
717
718
719
720
721
722
723
724
725
726
727
728
729
730
731
732
733
734
735
736
737
738
739
740
741
742

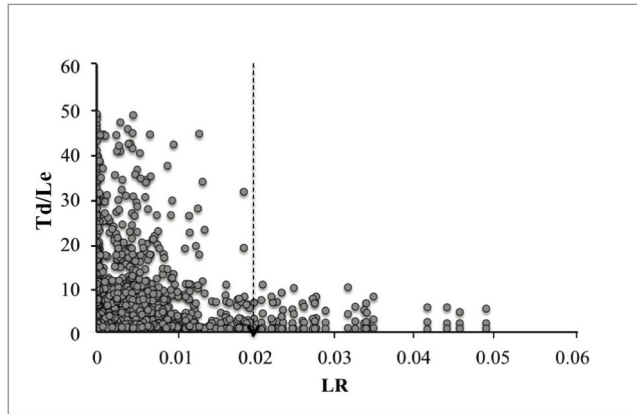
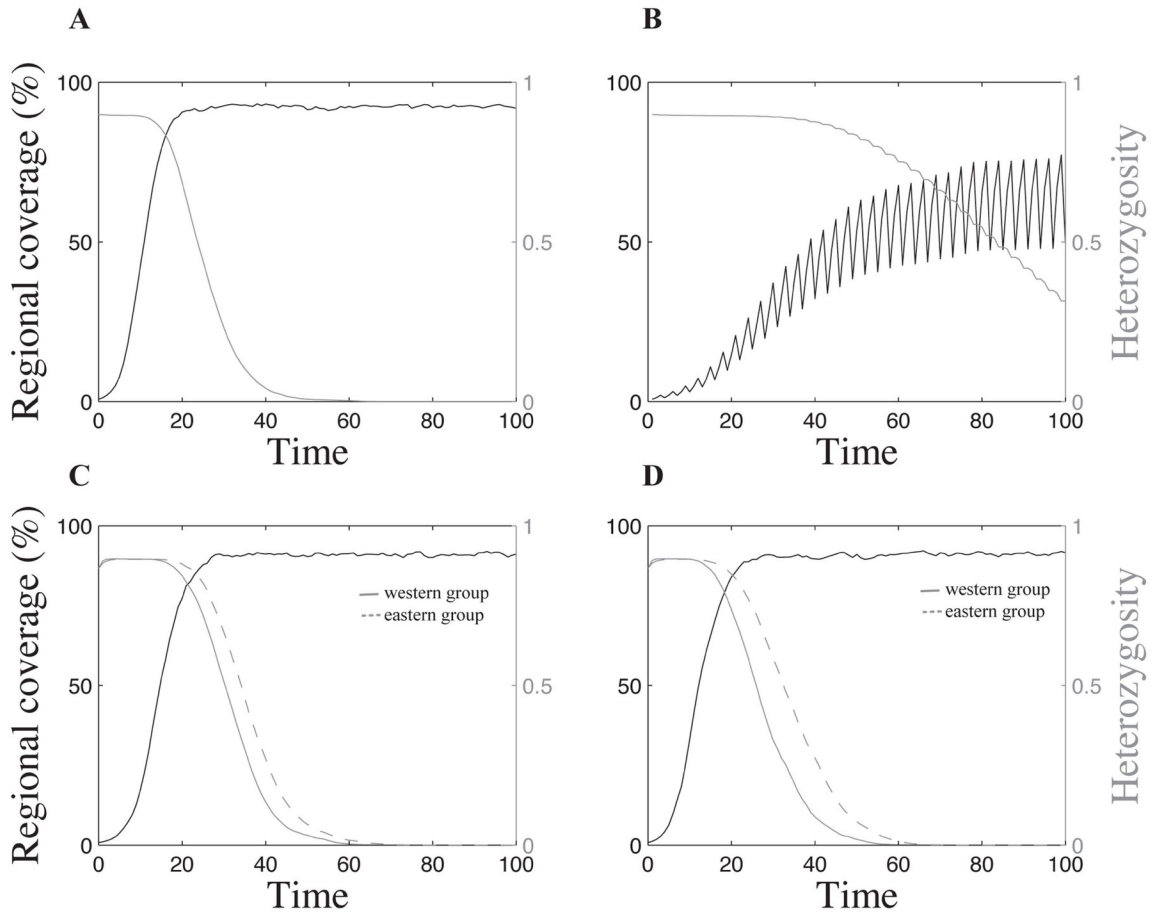


Figure 6. Relationship between local retention (LR; defined as the proportion of larvae produced in one population that remain in the same population) and the number of population turnovers to start losing genetic diversity (T_d/L_e), in a metapopulation over time. Values correspond to 20 connectivity matrices, and species with three different life expectancies (2, 5, and 20 years). Dashed arrow indicates the threshold at which the effect of LR on T_d/L_e begins to decrease.



744
 745 Figure 7. Effect of fluctuations in local population stability on heterozygosity over time.
 746 Scenarios: (a) Simulates gene flow among all of the populations forming a metapopulation
 747 with constant recruitment success every year. (b) Simulates recruitment failure (no
 748 recruitment) every 3 years. (c) Simulates the loss of four source sites (sites 17–20) in the
 749 metapopulation, while keeping recruitment success constant every year. (d) Simulates the
 750 loss of one key population (site 21) for maintaining genetic connectivity in the
 751 metapopulation.

752
 753
 754
 755
 756
 757
 758
 759
 760
 761
 762

